Error-Ellipse-Resampling-Based Particle Filtering Algorithm for Target Tracking

Xinxin Wang, Cheng Xu, *Member, IEEE*, Shihong Duan, and Jiawang Wan

***Abstract*—In this paper, an error-ellipse-resampling-based particle filter (EER-PF) algorithm is proposed for target tracking in wireless sensor networks. In order to improve the effectiveness of the particles, in the process of resampling, the error ellipse of different confidence levels is established according to the error covariance matrix of particles. The particles are divided into different levels based on the geometrical position, and then the particles are screened and optimized. The effectiveness of the proposed method in a cumulative error optimization was verified by comparing with the performance of posterior Cramér-Rao lower bound (PCRLB). Experimental results show that the proposed algorithm can effectively solve the problem of sample degeneracy and impoverishment, and has higher positioning accuracy.**

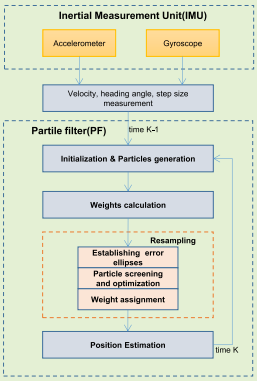

***Index Terms*—Particle filter (PF), error ellipse, resampling, posterior Cramér-Rao lower bound (PCRLB), cumulative error optimization.**

I. Introduction

AS ONE of the research hotspots of wireless sensor networks, the positioning and tracking of moving targets have a wide range of applications in pedestrian navigation [1], emergency search and rescue [2], and so on. Generally, to accomplish the target tracking in wireless sensor networks, two basic steps are required: 1) obtaining the target node's wireless feature parameters about its location; 2) perform the localization algorithm to complete the determination of target position.

Manuscript received December 14, 2019; revised January 14, 2020; accepted January 17, 2020. Date of publication January 21, 2020; date of current version April 16, 2020. This work was supported in part by the National Key Research and Development Program of China under Grant 2016YFB0700503, in part by the National Postdoctoral Program for Innovative Talents of China under Grant BX20190033, in part by the National Natural Science Foundation of China (NSFC) under Grant 61671056, and in part by the CERNET of China through CERNET Innovation Project under Grant NGII20160304. The associate editor coordinating the review of this article and approving it for publication was Dr. Ashish Pandharipande. *(Xinxin Wang and Cheng Xu are co-first authors.) (Corresponding author: Cheng Xu.)*

Xinxin Wang, Shihong Duan, and Jiawang Wan are with the School of Computer and Communication Engineering, University of Science and Technology Beijing, Beijing 100083, China, and also with the Beijing Key Laboratory of Knowledge Engineering for Materials Science, Beijing 100083, China.

Cheng Xu is with the School of Computer and Communication Engineering, University of Science and Technology Beijing, Beijing 100083, China, also with the Beijing Key Laboratory of Knowledge Engineering for Materials Science, Beijing 100083, China, and also with Shunde Graduate School, University of Science and Technology Beijing, Beijing 100083, China (e-mail: xucheng@ustb.edu.cn).

Digital Object Identifier 10.1109/JSEN.2020.2968371

In terms of location information parameter acquisition, Global Positioning System (GPS) [3] can achieve high-precision outdoor positioning, but it is greatly affected by signal conditions in densely populated areas such as indoors. In order to compensate for the high-precision positioning requirements under the above conditions, wireless positioning technology in local area networks is widely applied, such as Received Signal Strength (RSS) [4], Time of Arrival (TOA) [5], [6], Time Difference of Arrival (TDOA) [5], Angle of Arrival (AOA) [7], etc. However, wireless signal transmission is greatly affected by factors such as multipath and non-line-of-sight (NLOS). The RSS transmission-oriented system cannot accurately estimate the signal transmission distance, resulting in poor positioning accuracy. AOA measurement relies on a high-precision smart antenna array, which makes it difficult to deploy. Thus, it cannot be used on a large scale. TOA- and TDOA-based positioning systems have higher measurement accuracy, but they are affected by multipath and NLOS. The deployment of the base stations needs to consider the influence of the relative geometric position. In addition, TDOA requires high-precision synchronization technology support, which may lead to a large communication overhead. In contrast, the moving target tracking method based on an Inertial Measurement Unit (IMU) does not need to deploy infrastructure and has the characteristics of low cost and high precision. It has been widely concerned and applied. However, in long-term, wide-range target positioning applications, due to the inherent cumulative error and drift problem of inertial sensors [8], the error increases with the increase of the use time, and

it is difficult to automatically recover. Therefore, how to use the data processing algorithm to optimize the cumulative error of IMU is an urgent problem to be solved in practical applications.

The cumulative error problem of IMU could be solved by filtering methods [9] in practical applications. In specific applications, system equations and measurement equations are usually nonlinear, which makes traditional Kalman Filter (KF) unusable. Moreover, the most classic method to solve nonlinear filtering problems is the Extended Kalman Filter (EKF). The EKF algorithm is a local linear optimization based on a nonlinear system model, which can obtain ideal filtering results for weakly nonlinear systems. For strong nonlinear systems, the EKF inevitably introduces more truncation errors, making the true nonlinear characteristics of the system unrecognizable. Another filter that solves the nonlinear filtering problem is the Unscented Kalman Filter (UKF), which is based on the algorithm framework of unscented transformation and EKF. Because UKF does not linearize the system model, it can reflect the characteristics of the whole system more realistically. However, UKF still does not apply to general non-Gaussian distribution models [9].

Aiming at this problem, with the proposed Bayesian principle-based Monte Carlo particle filter (PF) [10], which overcomes the requirements of traditional Kalman filter for linear and Gaussian distribution systems. Particle filtering is a sequential process of state estimation. The iterative updating method of approximating the posterior distribution by a large number of particles (samples) avoids the problem that the required integral operation is difficult. Most of them are based on the following three steps: 1) predicting, generating a new set of particles; 2) updating, calculating particle weights; 3) resampling, rescreening the set of particles. However, particle filtering faces the problem of sample degeneracy and sample impoverishment in the resampling recursive process [11], [12]. Existing research has proposed many improved resampling algorithms, such as stratified resampling [11] and systematic resampling [12]. Both algorithms implement resampling based on layered ideas. Stratified resampling generates random numbers independently in each stratum, while systematic resampling chooses only one uniform random number and adds it to the ordered set. Thus, the samples of the systematic resampling are no longer independent and at the same position in the stratum. After a series of iterations, the filtered particle set will be reduced, which will cause most of the weights to be occupied by a few particles. As a result, the final state estimation result is not ideal. Therefore, how to solve the problem of sample degeneracy and impoverishment is a key to improve the accuracy of target tracking based on particle filter.

In summary, in this paper, we propose an error-ellipse-resampling-based particle filtering (EER-PF) method for target tracking, considering the geometric position distance between particles, and resampling at the different levels. The main contributions of this paper are listed as follows:

- Particle filter is used to optimize the measurement information of the IMU. The step size, velocity, and heading angle of the target node can be obtained by an IMU. The random walk model [13] is investigated to simulate the motion of target nodes and defines the state transition equation.
- To improve the problem of sample degeneracy and impoverishment, the concept of error ellipse is introduced to improve the resampling process. Different error ellipses are constructed according to covariance of potential particles at a certain moment. The overall particle set is divided into three levels, namely negligible particles, moderate particles, and dominating particles. In order to complete the screening and optimization of the particles, we will discard the negligible particles. Furthermore, the moderate particles and the dominating particles will be retained and copied, respectively.
- The cumulative error problem of an IMU is considered and verified with comparison of its lower bound. Posterior Cramér-Rao lower bound based on IMU method is derived, so as to verify the effectiveness of the proposed particle filter tracking algorithm in the aspect of cumulative error correction.

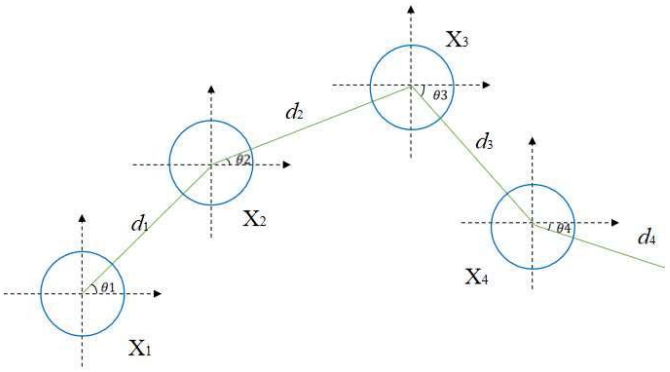

Fig. 1. An example trajectory of a randomly walking target node: 3 steps from a known initial position, while step size d_k and heading angle θ_k can be obtained by an inertial measurement unit.

The remainder of this paper is organized as follows: Section II gives the problem definition and the state equation of the system. Section III describes the detailed filtering method and the proposed error-ellipse-resampling process. Section IV shows the experimental results and analysis. Conclusions are drawn in Section V.

II. Problem Formulation

Fig. 1 illustrates the random motion process of the single target node. The state parameter of the target node at time k is represented by $X_k \triangleq [x_k, y_k]$, $k \in [0, K-1]$, where x_k and y_k denotes the positional information of the target node in a two-dimensional Cartesian coordinate system. Therefore, all state information of the target node is counted as a vector $X = [X_0^T, X_1^T, \cdots, X_{K-1}^T]^T$. In general, the knowledge of a random walk model can be modeled as a Gauss-Markov process [13]:

$$X_{k+1} = X_k + T_k v_k \tag{1}$$

where T_k represents the motion period of the target node from time k to time $k+1$, and v_k denotes the velocity from time

k to time $k+1$. Both the step size and velocity of the target node can be obtained from the accelerometer measurement:

$$\hat{d}_k = d + u_k, u_k \sim N(0, \gamma_{1,k}^2) \tag{2}$$

where d represents the true distance between the positions of time k and $k+1$, i.e.,

$$d = \sqrt{(x_{k+1} - x_k)^2 + (y_{k+1} - y_k)^2} \tag{3}$$

and u_k is the step noise that obeys the Gaussian distribution with a mean of 0 and a covariance of $\gamma_{1,k}^2$. Thus, the vector $\hat{d} = [\hat{d}_0, \hat{d}_1, \cdots, \hat{d}_{K-1}]^T$ reflects the step size information.

$$\hat{v}_k = v + r_k, r_k \sim N(0, \gamma_{2,k}^2) \tag{4}$$

where v represents the actual walking velocity of the target node, and r_k is the velocity noise that obeys the Gaussian distribution with a mean of 0 and a covariance of $\gamma_{2,k}^2$. $\hat{v}$ is introduced to collect $\hat{v}_k$, given by $\hat{v} = [\hat{v}_0, \hat{v}_1, \cdots, \hat{v}_{K-1}]^T$. The heading angle of the target node can be measured by the gyroscope:

$$\hat{\theta}_k = \theta_k + \eta_k, \eta_k \sim N(\kappa, \gamma_{3,k}^2) \tag{5}$$

where θ_k is the actual horizontal angle, i.e.,

$$\theta_k = arctan \frac{y_{k+1} - y_k}{x_{k+1} - x_k} \tag{6}$$

and η_k is the heading angle noise that obeys the Gaussian distribution with a mean of κ and a covariance of $\gamma_{3,k}^2$. Thus, the vector $\hat{\theta} = [\hat{\theta}_0, \hat{\theta}_1, \cdots, \hat{\theta}_{K-1}]^T$ reflects the heading angle information during the motion of the target node. According to the standards of random walk model, we assume that the target node has a motion period of $1s$ and maintains uniform motion. Then, the state transition equation of the target tracking by the PF algorithm is expressed as:

$$\begin{bmatrix} x_k^i \\ y_k^i \end{bmatrix} = \begin{bmatrix} x_{k-1}^i + \hat{v}_k^i \cos\hat{\theta}_k^i \\ y_{k-1}^i + \hat{v}_k^i \sin\hat{\theta}_k^i \end{bmatrix} + \begin{bmatrix} \sigma_x \\ \sigma_y \end{bmatrix}, \sigma_x, \sigma_y \sim N(\tau, \varepsilon^2) \tag{7}$$

where $[x_k^i, y_k^i]^T$ and $[x_{k-1}^i, y_{k-1}^i]^T$ represent the position of particle i at time k and $k-1$, respectively. $\hat{v}_k^i$ and $\hat{\theta}_k^i$ are the velocity and heading angle obtained by particle i at time k, respectively. The variables σ_x and σ_y are noises on the horizontal and vertical coordinates, which obey the Gaussian distribution with a mean of τ and a covariance of ε^2. The moving target node can obtain a position estimation for each state by calculating a posteriori probability density function $p(Z_k|X_k)$, where $Z_k = [\hat{d}_k, \hat{v}_k, \hat{\theta}_k]$ is an observation vector.

III. Particle Filter Algorithm

In the random walk model for target tracking, the step size, velocity, and heading angle information of a single target motion can be measured by an IMU. However, in practical applications, the distribution of these mentioned data may be non-Gaussian. Furthermore, particle filter can be well fit for the non-Gaussian nonlinear target tracking process. In this paper, we propose an error-ellipse-resampling-based PF algorithm (EER-PF). We introduce the concept of error ellipse to improve the resampling process, so as to overcome the problem of sample degeneracy and impoverishment.

A. Initialization and Weights Calculation

The PF completes the estimation of the state X_k by updating a set of random measurements $[X_{1:k}^i, w_k^i]_{i=1}^N$, which consist of N particles X_k^i at time k and the corresponding weight w_k^i. The state estimation can be calculated from this set of random measurements. When the quantity of samples is large enough, this estimation for the state will approximate the posterior probability density function $p(X_{1:k}|Z_{1:k})$ of the unknown distribution $X_{1:k}$. In the initialization phase, the N particles are initialized using the following formula:

$$\begin{bmatrix} x_0^i \\ y_0^i \end{bmatrix} = \begin{bmatrix} \hat{x}_0 \\ \hat{y}_0 \end{bmatrix} + \begin{bmatrix} \sigma_x \\ \sigma_y \end{bmatrix} \tag{8}$$

where $[\hat{x}_0, \hat{y}_0]^T$ is the initial position of the target to be tracked, and σ_x and σ_y are Gaussian noises in the horizontal and vertical directions, respectively. In the Bayesian setup, there are two frameworks for forecasting and updating. It is assumed that the state transition process obeys the first-order Markov model, namely $p(X_k|X_{1:k-1}) = p(X_k|X_{k-1})$. Then in the prediction phase, the prior probability density function $p(X_k|Z_{1:k-1})$ can be calculated from the filter distribution $p(X_{k-1}|Z_{1:k-1})$ at time $k-1$:

$$p(X_k|Z_{1:k-1}) = \int \overbrace{p(X_k|X_{k-1})}^{system\ model} \overbrace{p(X_{k-1}|Z_{1:k-1})}^{previous\ posterior} dX_{k-1} \tag{9}$$

where $p(X_{k-1}|Z_{1:k-1})$ is assumed to be known and $p(X_k|Z_{1:k-1})$ is determined by equation (7). In the update phase, the posterior probability density function is updated by a new set of measured values Z_k, namely

$$p(X_k|Z_{1:k}) = \frac{\overbrace{p(Z_k|X_k)}^{measurement\ model} \overbrace{p(X_k|Z_{1:k-1})}^{current\ prior}}{\underbrace{p(Z_k|Z_{1:k-1})}_{normalized\ constant}} \tag{10}$$

where $p(Z_k|X_k)$ is the likelihood function defined by the measurement equation [14] and $p(Z_k|Z_{1:k-1})$ is the normalized constant. In fact, the posterior probability density function is not known, so Monte Carlo sampling is introduced to sample a set of random weighted samples from the state space of the known distribution instead of the posterior probability distribution, i.e., $X_k^i \sim q(X_k^i|X_{k-1}^i, Z_k)$, where $q(\cdot)$ is the importance probability density function [15]. Then, the weight is initialized to $1/N$ and updated by:

$$w_k^i \sim w_{k-1}^i \frac{p(Z_k|X_k^i)p(X_k^i|X_{k-1}^i)}{q(X_k^i|X_{k-1}^i, Z_k)} \tag{11}$$

The transitional prior probability density function is usually selected as the importantce density, that is $q(X_k^i|X_{i-1}^i, Z_k) = p(X_k^i|X_{k-1}^i)$ [15]. Followed by normalization $\tilde{w}_k^i = w_k^i / \sum_{i=1}^N w_k^i$. Finally, the approximate posterior probability density function can be calculated as:

$$p(X_k|Z_{1:k}) \approx \sum_{i=1}^{N} \tilde{w}_k^i \delta(X_k - X_k^i) \tag{12}$$

where w_k^i and X_k^i are the weight and the state of the particle i, respectively, and $\delta(\cdot)$ is the Dirac delta function. When $N \to \infty$, the approximation approaches the true posterior density.

B. Resampling Method for Particle Filtering

On one hand, most of the weights are concentrated on a few particles as the iteration proceeds, which is called sample degeneracy. These degraded particles will also affect the final estimation results. On the other hand, sample impoverishment is due to the fact that most of the negligible particles are discarded during the iteration, which resulting in loss of sample diversity. In order to solve these problems, a method of particle grading using an error ellipse is described in this section.

1) Error Ellipse: The error ellipse, also known as the confidence ellipse, is derived from the interval estimation of the coordinate parameters. Some concepts in the interval estimation: when estimating the interval s (the range of the estimated scale), if a small probability β is given in advance, an interval (s_1, s_2) can be found to satisfy:

$$p(s_1 < s < s_2) = 1 - \beta \tag{13}$$

Then the interval (s_1, s_2) is called the confidence interval of the scale s, and s_1 and s_2 are called confidence limits (or critical values); $s \le s_1$ and $s \ge s_2$ are called negative domains; probability β is called significance level (or risk), and $1 - \beta$ is called confidence level (or probability). In the study of this paper, we consider the two-dimensional covariance matrix of N particles at time k:

$$D = \begin{bmatrix} cov(x,x) & cov(x,y) \\ cov(y,x) & cov(y,y) \end{bmatrix} \tag{14}$$

where $cov(x,x)$ and $cov(y,y)$ are the variances in the x-axis and y-axis directions, respectively. However, data showing relevance can be obtained by extending the concept of variance:

$$cov(x,y) = E[(x - E(x))(y - E(y))] \tag{15}$$

If x is positively related to y, then y and x are also positively correlated, i.e., $cov(x,y) = cov(y,x)$. Therefore, the covariance matrix is always a symmetric matrix with a variance on the diagonal and a covariance on the off-diagonal. When the error covariance matrix is introduced, the equation of error ellipse, whose center is not at the origin, is expressed as:

$$s = \frac{(x - x_p)^2}{\lambda_1} + \frac{(y - y_p)^2}{\lambda_2} \tag{16}$$

where λ_1 and λ_2 are the largest and smallest eigenvectors of the covariance matrix D, respectively. (x_p, y_p) is the predicted position and s is the size of the ellipse. Furthermore, when the ellipse is tilted, the angle α between the x-axis and the y-axis is described as

$$\alpha = arctan\frac{\lambda_1(y)}{\lambda_2(x)} \tag{17}$$

Assuming the rotated coordinates are (x', y'), then

$$\begin{cases} x' = x\cos\alpha - y\sin\alpha \\ y' = x\sin\alpha + y\cos\alpha \end{cases} \tag{18}$$

The formula after replacing (x, y) with (x', y') is expressed as

$$\begin{cases} x = x'\cos\alpha + y'\sin\alpha \\ y = -x'\sin\alpha + y'\cos\alpha \end{cases} \tag{19}$$

Substitute the formula (19) into (16), then the error ellipse is formalized as:

$$s = \frac{((x' - x_p)\cos\alpha + (y' - y_p)\sin\alpha)^2}{\lambda_1} + \frac{(-(x' - x_p)\sin\alpha + (y' - y_p)\cos\alpha)^2}{\lambda_2} \tag{20}$$

In summary, the error ellipse constraint is

$$s \ge \frac{((x' - x_p)\cos\alpha + (y' - y_p)\sin\alpha)^2}{\lambda_1} + \frac{(-(x' - x_p)\sin\alpha + (y' - y_p)\cos\alpha)^2}{\lambda_2} \tag{21}$$

2) Particle screening and optimization: Fig. 2 depicts a resampling process for particle sets based on error ellipses. Two different confidence levels (confidence probabilities) are established. During the resampling process, N potential particles are divided into three different levels by geometric positions. The particles outside the outer ellipse are N_l negligible particles which will be discarded; the particles located in the middle of the two ellipses are regarded as the moderate particles, and these particles will be reserved; N_h dominating particles in the inner ellipse will be duplicated. During the duplication process, since the rounding operation may lead to the duplication times of particles to be less than 1, the first $N_t = (N_l - \lfloor N_l/N_h \rfloor N_h)$ dominating particles are duplicated $c_1 = \lfloor N_l/N_h \rfloor + 2$ times, then the remaining dominating particles $N_t - N_l$ are duplicated $c_2 = \lfloor N_l/N_h \rfloor + 1$ times. After all particles have performed the duplication operation, the quantity of particles is still N. The selected set of particles will also be used as initial input for the next iteration.

3) Weight assignment and estimation results update: During the resampling process, due to the discarding and duplication of some particles, the weights of the discarded particles are reassigned to the particles being duplicated. However, the number of particles after screening and replication is still N. The weights are redistributed using the following equation:

$$\varpi_k^i = \begin{cases} (1 - M)/(N_l + N_h), & s_k^i < s_2 \\ \tilde{w}_k^i, & s_1 \le s_k^i \le s_2 \\ 0, & s_k^i > s_1 \end{cases} \tag{22}$$

where M is the sum of the weights of the moderate particles, N_l and N_h are the quantity of negligible particles and dominating particles, respectively. The value s_k^i is calculated by formula (19) for particle i at time k. Finally, the estimated results of the state are updated by the weighted average:

$$\begin{cases} x_k = \sum_{i=1}^{N} \varpi_k^i x_k^i \\ y_k = \sum_{i=1}^{N} \varpi_k^i y_k^i \end{cases} \tag{23}$$

The overall resampling algorithm is described as shown in Algorithm 1.

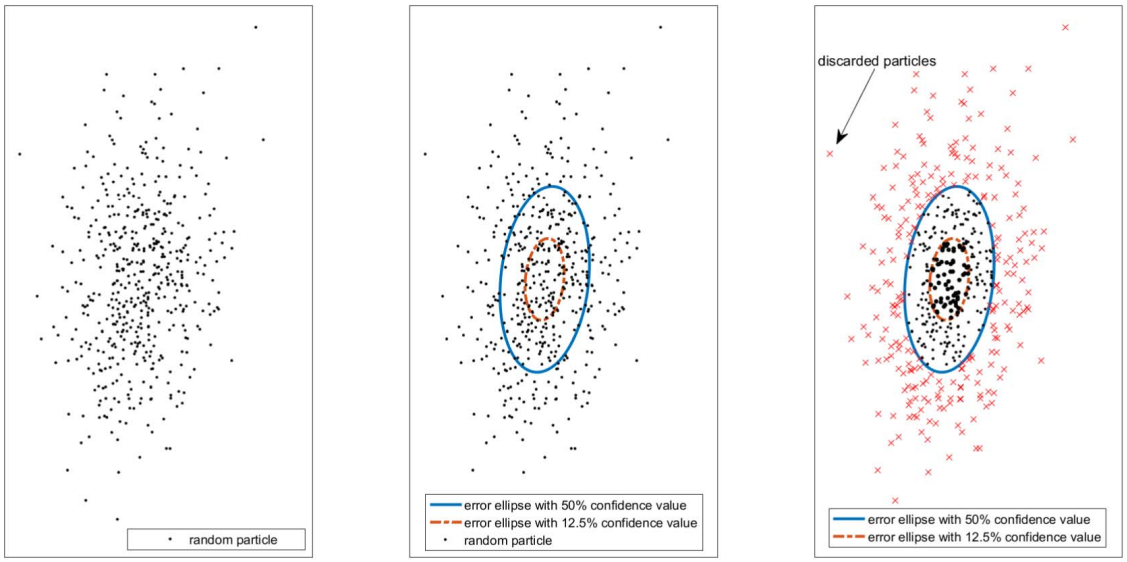

Fig. 2. An example of a resampled particle screening process: a) shows the initial distribution of the particles. b) two different confidence level ellipse (50% confidence probability and 12.5% confidence probability) based on the covariance matrix of the particle set. c) Screening results for particles of different levels. The red particles could be removed and the bold points are copied, to emphasize the high weight particles and reduce the low weight ones.

Algorithm 1 Error-Ellipse-Resampling Algorithm (EER-PF)

Input: $\left\{X_k^i, \tilde{\omega}_k^i\right\}_{i=1}^N \leftarrow$ status, weight information
Output: $\left\{indexh, indexm, M, c^{(m)}\right\} \leftarrow$ resampling index, weight sum, number of copies
for $i \leftarrow 1, N$ **do**
  $s_k^i \leftarrow ellipse(X_k^i, (x_p, x_p)) \triangleright formula(20)$;
  if $s_k^i > s_1$ **then**
    $indexl(N_l) \leftarrow i$;
    $N_l \leftarrow N_l + 1$;
  else if $s_k^i < s_2$ **then**
    $indexh(N_h) \leftarrow i$;
    $N_h \leftarrow N_h + 1$;
  else
    $M \leftarrow M + \tilde{\omega}_k^i$;
  end if
end for
$N_t \leftarrow N_l - \lfloor N_l / N_h \rfloor * N_h$;
for $m \leftarrow 1, N_h$ **do**
  if $m \leq N_t$ **then**
    $c^{(m)} = \lfloor N_l / N_h \rfloor + 2$;
  end if
  $c^{(m)} = \lfloor N_l / N_h \rfloor + 1$;
end for

IV. Experimental Results and Analysis

In order to verify the effectiveness of EER-PF algorithm in single target tracking process, we simulate the random walking process and location estimation of a single target through MATLAB software. The target node moves at a constant speed in a two-dimensional coordinate system of 50m × 50m, and the sampling interval of each experiment is 1s. The initial position (x_0, y_0) of the target node and the moving heading angle θ are randomly generated. The step d of each walk is 2m, and the step noise u_k obeys a Gaussian distribution with a mean of 0 and a variance of 0.1m^2 ($\gamma_{1,k}^2 = 0.1\text{m}^2$). The velocity of each walk is set to 2m/s, and the velocity noise r_k obeys the Gaussian distribution with a mean of 0 and a variance of 0.1m/s ($\gamma_{2,k}^2 = 0.1\text{m/s}^2$). The angle noise η obeys a Gaussian distribution with a mean of 10° and a variance of 0.1 ($\kappa = 10°$, $\gamma_{3,k}^2 = 0.01$). The random jitters σ_x and σ_y obeys the Gaussian distribution with a mean of 0.1m and a variance of 0.1m^2 ($\tau = 0.1\text{m}$, $\varepsilon^2 = 0.1\text{m}^2$). The positioning error ρ of the random walk model is calculated from the Euclidean distance between the predicted position and the real position:

$$\rho = \sqrt{\left(x_p - x_t\right)^2 + \left(y_p - y_t\right)^2} \tag{24}$$

A. Posterior Cramér-Rao Lower Bound

PCRLB is often used to provide a theoretical lower limit on system performance [16]. Under the premise of considering time domain information, the joint probability function is defined as:

$$p\left(\hat{d}, \hat{v}, \hat{\theta}, \hat{X}\right) = p\left(\hat{d}_0 | X_0\right) \prod_{k=1}^{K} p\left(\hat{v}_k | X_{k-1}, X_k\right) \cdot p\left(\hat{\theta}_k | X_{k-1}, X_k\right) p\left(\hat{d}_k | X_k\right) \tag{25}$$

The root mean square error (RMSE) of $\hat{X}_k$ is limited by the Fisher information matrix:

$$E\left\{\left(\hat{X}_k - X_k\right)^2\right\} \geq \sqrt{tr\left(J(X_k)^{-1}\right)} \tag{26}$$

In the above formula, $tr(\cdot)$ stands for the trace of the matrix, and the Fisher information matrix J is expressed as:

$$J(X) = E_{\hat{d},\hat{v},\hat{\theta}}\left\{-\Delta_X^X \ln p\left(\hat{d},\hat{v},\hat{\theta},\hat{X}\right)\right\} \tag{27}$$

where $\Delta_b^a = \nabla_b \nabla_a^T$ is the second-order derivative and $\nabla_a = [\frac{\partial}{\partial a_1}, \frac{\partial}{\partial a_2}, \cdots, \frac{\partial}{\partial a_M}]^T$ is defined as the gradient vector of a. Therefore, the joint probability density p_k at the state k can be defined as:

$$p_k = p\left(\hat{d}_{0:k}, \hat{v}_{0:k}, \hat{\theta}_{0:k}, \hat{X}_{0:k}\right) \tag{28}$$

where $\hat{d}_{0:k} = (\hat{d}_0, \hat{d}_1, \cdots, \hat{d}_K)$, $\hat{v}_{0:k} = (\hat{v}_0, \hat{v}_1, \cdots, \hat{v}_K)$, $\hat{\theta}_{0:k} = (\hat{\theta}_0, \hat{\theta}_1, \cdots, \hat{\theta}_K)$, $\hat{X}_{0:k} = (\hat{X}_0, \hat{X}_1, \cdots, \hat{X}_K)$ are expressed as a set of step size, velocity, heading angle, and target coordinate vectors from the initial state to the state k. We assume that the state vector can be expressed as $X_k = [X_{0:k-1}^T, X_k^T]^T$, then the Fisher information matrix for $X_{0:k}$ can be written as:

$$\begin{aligned} J(X_{0:k}) &= \begin{bmatrix} E\left\{-\Delta_{X_{0:k-1}}^{X_{0:k-1}} \ln p_k\right\} & E\left\{-\Delta_{X_{0:k-1}}^{X_k} \ln p_k\right\} \\ E\left\{-\Delta_{X_k}^{X_{0:k-1}} \ln p_k\right\} & E\left\{-\Delta_{X_k}^{X_k} \ln p_k\right\} \end{bmatrix} \\ &= \begin{bmatrix} A_k & B_k \\ B_k^T & C_k \end{bmatrix} \end{aligned} \tag{29}$$

where A_k, B_k, B_k^T, C_k represent the Fisher information matrix $J(X_{0:k-1}, X_{0:k-1})$, $J(X_k, X_{0:k-1})$, $J(X_{0:k-1}, X_k)$, $J(X_k, X_k)$, respectively. According to the literature [17], the sub-matrix can be obtained by the pseudo-inverse of the matrix, i.e.,

$$J_k = C_k - B_k^T A_k^{-1} B_k \tag{30}$$

Therefore, the joint probability density p_{k+1} at the state $k+1$ is defined as:

$$\begin{aligned} p_{k+1} = p_k p\left(\hat{d}_{k+1}|X_{k+1}\right) p\left(\hat{v}_{k+1}|X_k, X_{k+1}\right) \\ \times p\left(\hat{\theta}_{k+1}|X_k, X_{k+1}\right) \end{aligned} \tag{31}$$

According to the joint probability density p_{k+1}, the Fisher information matrix $J(X_{0:k+1})$ of state $k+1$ can be solved:

$$J(X_{0:k+1}) = \begin{bmatrix} A_k & B_k & 0 \\ B_k^T & C_k + H_k^{11} & H_k^{12} \\ 0 & H_k^{12} & \phi_{k+1} + H_k^{22} \end{bmatrix} \tag{32}$$

where H_k^{11}, H_k^{12} and H_k^{22} reflect the posterior information from state k to state $k+1$,

$$\begin{aligned} H_k^{11} = E_{\hat{v},\hat{\theta}}\Big\{-\Delta_{X_k}^{X_k} \ln p\left(\hat{v}_{k+1}|X_k, X_{k+1}\right) \\ \times p\left(\hat{\theta}_{k+1}|X_k, X_{k+1}\right)\Big\} \end{aligned} \tag{33}$$

$$\begin{aligned} H_k^{12} = E_{\hat{v},\hat{\theta}}\Big\{-\Delta_{X_k}^{X_{k+1}} \ln p\left(\hat{v}_{k+1}|X_k, X_{k+1}\right) \\ \times p\left(\hat{\theta}_{k+1}|X_k, X_{k+1}\right)\Big\} = \left(H_k^{21}\right)^T \end{aligned} \tag{34}$$

$$\begin{aligned} H_k^{22} = E_{\hat{v},\hat{\theta}}\Big\{-\Delta_{X_{k+1}}^{X_{k+1}} \ln p\left(\hat{v}_{k+1}|X_k, X_{k+1}\right) \times \\ \times p\left(\hat{\theta}_{k+1}|X_k, X_{k+1}\right)\Big\} \end{aligned} \tag{35}$$

where ϕ_{k+1} is the positional information defined by the measurement equation, i.e.,

$$\phi_{k+1} = E_{\hat{d}_{k+1}}\left\{-\Delta_{X_{k+1}}^{X_{k+1}} \ln p\left(\hat{d}_{k+1}|X_{k+1}\right)\right\} \tag{36}$$

Then, the Fisher information matrix of state $k+1$ can be derived from $J(X_{0:k+1})$ and J_k,

$$\begin{aligned} J_{k+1} &= \phi_{k+1} + H_k^{22} - \begin{bmatrix} 0 & H_k^{21} \end{bmatrix} \begin{bmatrix} A_k & B_k \\ B_k^T & C_k + H_h^{11} \end{bmatrix} \begin{bmatrix} 0 \\ H_k^{12} \end{bmatrix} \\ &= \phi_{k+1} + H_k^{22} - H_k^{21}\left(J_k + H_k^{11}\right)^{-1} H_k^{12} \end{aligned} \tag{37}$$

Since the velocity error r_k and the heading angle error η_k obey the Gaussian distribution, the following conclusions can be drawn:

$$H_k^{11} = H_k^{12} = H_k^{22} = H_k \tag{38}$$

$$H_k = \frac{\xi_{\hat{v}_{k+1}}(\theta_{k+1})}{\gamma_{2,k}^2} + \frac{\xi_{\hat{\theta}_{k+1}}(\theta_{k+1})}{\gamma_{3,k}^2 v_{k+1}^2} \tag{39}$$

$$\xi_{\hat{v}_{k+1}}(\theta_{k+1}) = \begin{bmatrix} \cos^2\theta_{k+1} & \cos\theta_{k+1}\sin\theta_{k+1} \\ \cos\theta_{k+1}\sin\theta_{k+1} & \sin^2\theta_{k+1} \end{bmatrix} \tag{40}$$

$$\xi_{\hat{\theta}_{k+1}}(\theta_{k+1}) = \begin{bmatrix} \sin^2\theta_{k+1} & -\cos\theta_{k+1}\sin\theta_{k+1} \\ -\cos\theta_{k+1}\sin\theta_{k+1} & \cos^2\theta_{k+1} \end{bmatrix} \tag{41}$$

Therefore, the posterior Fisher information matrix:

$$J_{k+1} = \phi_{k+1} + H_k - H_k(J_k + H_k)^{-1} H_k \tag{42}$$

The above formula can be further simplified to

$$J_{k+1} = \phi_{k+1} + \left(H_k^{-1} + J_k^{-1}\right)^{-1} \tag{43}$$

where $\phi_k + 1$ is the position information of the state $k+1$ defined by the measurement equation, and H_k reflects the information based on the IMU. Finally, we can iteratively calculate the Fisher information matrix at each moment by equation (43) to get the corresponding PCRLB. The Fisher information matrix at the initial moment can be obtained from the ranging information at the initial moment, that is, $J_0 = \phi_0$.

B. Experimental Results and Performance Analysis

In order to verify the effectiveness of our proposed EER-PF algorithm for cumulative error correction, we chose unresampled algorithm, stratified resampling algorithm [11], and systematic resampling algorithm [12] as comparison algorithms, and compare their performance in location tracking experiments. Furthermore, their positioning errors are compared with PCRLB under a single IMU method. The experiment simulates a random walk process. The target node travels 100 steps from the initial position and generates the real trajectory of the target node motion. The proposed EER-PF algorithm generates 4000 particles near the initial position. After that, the algorithm will predict the position of the target node for each walk, and then generate the predicted trajectory of the target node motion. The Euclidean distance between the predicted position and the real position during the progress of the target node is statistically obtained, and the error distribution curves of the above-mentioned algorithms are obtained.

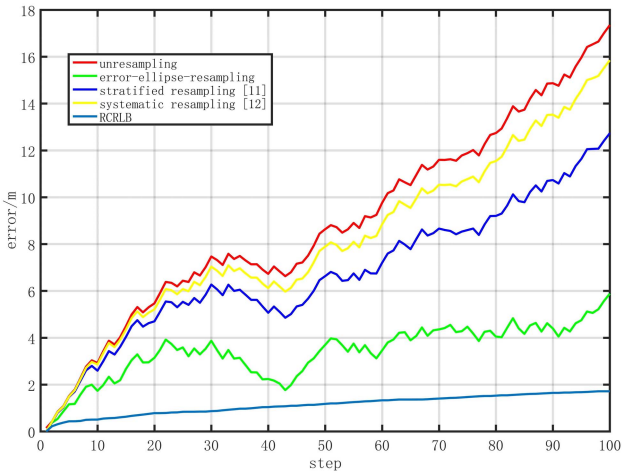

Fig. 3. Schematic diagram of cumulative error statistics.

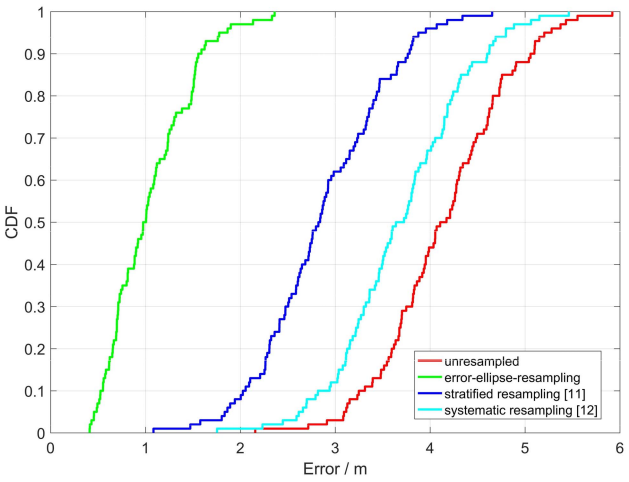

Fig. 5. Cumulative function distribution curve.

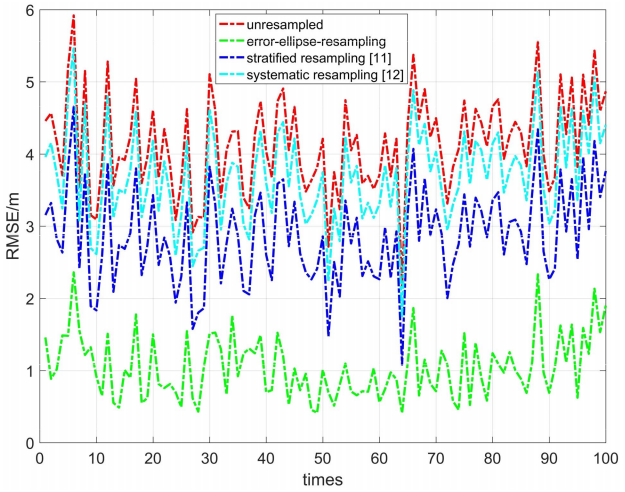

Fig. 4. Schematic diagram of statistical distribution of root mean square error in 100 random walk experiments.

Fig. 3 shows the cumulative errors of the four location tracking algorithms in a random walk experiment. It can be seen that the positioning error of the four tracking algorithms will increase with the movement of the target node, which confirms the cumulative error and drift of the IMU. The position estimation error of the proposed EER-PF algorithm is closer to the theoretical lower limit. The maximum difference between the unresampled algorithm and the PCRLB is 15.62m, the maximum difference between the systematic resampling algorithm and the PCRLB is 14.10m, and the maximum difference between the stratified resampling algorithm and the PCRLB is 10.90m. By contrast, the maximum difference between the proposed EER-PF algorithm and the PCRLB is 2.67m. The results show that the EER-PF algorithm proposed in this paper can effectively suppress the increase of cumulative error, and improve the positioning accuracy of the IMU-based tracking method.

In order to verify the high precision and high stability of the proposed PF algorithm, we repeated the above random walk experiment 100 times. In each experiment, the target node randomly walks 100 steps and uses different algorithms to predict the true position of the single target random walk. Finally, the RMSE and variance of the experiment were recorded.

The RMSE distribution curve of 100 random walk experiments is depicted in Fig. 4. It can be seen that the RMSE curve of the unresampled algorithm is significantly higher than other methods because the resampling process is a key step of particle filtering, which can improve the effectiveness of the particles. The algorithm based on error-ellipse-resampling proposed in this paper can achieve higher positioning accuracy. Table I shows the variance extremes and the average positioning error of different algorithms for positioning tracking, where EER-PF has a maximum variance is 5.63m^2 and a minimum variance is 0.17m^2. Therefore, the proposed algorithm has higher stability in the tracking process. The algorithm proposed in this paper can achieve a positioning accuracy of 1.05m. The cumulative error distribution results in Fig. 5 show that the proposed algorithm has a 50% probability of better than 1m and a 97% probability of better than 2m. The positioning errors of the other three algorithms are all above 1 m, it's confirmed that the proposed error-ellipse-resampling PF algorithm can achieve high-precision single target motion tracking.

C. Comparison of Confidence Level and Particle Quantity

In order to compare the influence of different confidence levels and particle numbers on the positioning accuracy of the PF algorithm, in this experiment, we used two sets of thresholds, the quantity of particles N and the confidence interval $(1-\beta_1, 1-\beta_2)$. We selected different particle numbers and confidence intervals, respectively, and used the EER-PF algorithm to track the movement of a single target. The results of the positioning error of the experiment under different parameters were counted. The RMSE is used to indicate the positioning accuracy of the algorithm. In addition, in order to compare the influence of different particle numbers on the execution time of the proposed PF algorithm, we define the time period from the input measurement value to the output positioning estimation result as the execution time.

TABLE I
ERROR COMPARISON OF DIFFERENT POSITIONING METHODS

Resampling method	Maximum variance (m^2)	Minimum variance (m^2)	Average error (m)
unresampled	35.41	4.70	4.15
stratified resampling	21.89	1.19	2.87
systematic resampling	30.13	3.11	3.67
EER-PF	**5.63**	**0.17**	**1.05**

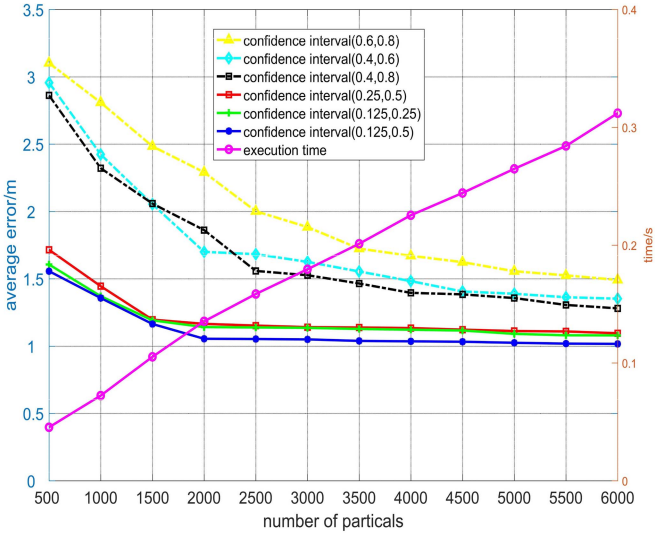

Fig. 6. Positioning accuracy and calculation time corresponding to different particle quantity and confidence intervals.

Fig. 6 shows the average positioning error distribution for target tracking using different particle quantity and confidence intervals. The number of particles is set to increase from 500 to 6000. It can be seen from the figure that when the confidence interval variable is the same, more particles will reduce the positioning error of the algorithm. Therefore, it is more appropriate to chose a confidence interval (0.125,0.5). In addition, the figure shows that the execution time of the algorithm increases by 0.025s as the number of particles increases by 500 each time. When the number of particles reaches 2000, the positioning error of the algorithm tends to be stable, so the number of particles is more suitable for 2000.

V. CONCLUSIONS

In this paper, we propose an EER-PF algorithm for target tracking. Generally, the target's coordinates are the most considerable information in practical applications. As far as EER-PF is concerned, the state vector can be muti-dimensional, and the others states variables such as heading angle and velocity could be auxiliary sub-vectors. As for the error ellipse method in EER-PF, it could be regarded as confidence interval in one-dimensional application, and generalized to error ellipsoid, and moreover, abstract ellipsoid in higher dimensional applications. We simulate the random walk process of a single target, experiments prove that the proposed EER-PF algorithm can effectively suppress the unrestricted increase of cumulative errors. In the resampling phase, the particle set is divided by a geometric position using the constraints of the error ellipse, and the particle set is reselected and copied. The problem of sample degeneracy and sample impoverishment of the PF algorithm is effectively improved. The experimental results confirm that the proposed algorithm can achieve a high-precision and high-stability tracking process. At the same time, the choice of confidence interval has a significant influence on the final estimation result. Choosing the appropriate confidence interval and particle quantity can effectively improve the positioning performance of the algorithm.

REFERENCES

[1] X. Xing, R. Zhou, and L. Yang, "The current status of development of pedestrian autonomous navigation technology," in *Proc. 26th Saint Petersburg Int. Conf. Integr. Navigat. Syst. (ICINS)*, Saint Petersburg, Russia, May 2019, pp. 1–3.

[2] Z. Uddin and M. Islam, "Search and rescue system for alive human detection by semi-autonomous mobile rescue robot," in *Proc. Int. Conf. Innov. Sci., Eng. Technol. (ICISET)*, Dhaka, Bangladesh, Oct. 2016, pp. 1–5.

[3] Y. Zhang, "A fusion methodology to bridge GPS outages for INS/GPS integrated navigation system," *IEEE Access*, vol. 7, pp. 61296–61306, 2019.

[4] L. Li, X. Guo, F. Xu, and F. Hu, "An accurate and calibration-free approach for RSS-based WiFi localization," in *Proc. IEEE 23rd Int. Conf. Digit. Signal Process. (DSP)*, Shanghai, China, Nov. 2018, pp. 1–5.

[5] Z. Guohui and W. Yang, "An approximately efficient estimator for moving source localization using multiple-time TDOA measurements," in *Proc. 14th IEEE Int. Conf. Signal Process. (ICSP)*, Beijing, China Aug. 2018, pp. 934–938.

[6] C. Xu, M. Ji, Y. Qi, and X. Zhou, "MCC-CKF: A distance constrained Kalman filter method for indoor TOA localization applications," *Electronics*, vol. 8, no. 5, p. 478, Apr. 2019.

[7] D. Zhang, Y. He, X. Gong, Y. Hu, Y. Chen, and B. Zeng, "Multitarget AOA estimation using wideband LFMCW signal and two receiver antennas," *IEEE Trans. Veh. Technol.*, vol. 67, no. 8, pp. 7101–7112, Aug. 2018.

[8] H. Ahmed and M. Tahir, "Improving the accuracy of human body orientation estimation with wearable IMU sensors," *IEEE Trans. Instrum. Meas.*, vol. 66, no. 3, pp. 535–542, Mar. 2017.

[9] W. Wang and P. G. Adamczyk, "Comparison of bingham filter and extended Kalman filter in IMU attitude estimation," *IEEE Sensors J.*, vol. 19, no. 19, pp. 8845–8854, Oct. 2019.

[10] N. Gordon, D. Salmond, and A. Smith, "Novel approach to nonlinear/non-Gaussian Bayesian state estimation," *IEE Proc. F Radar Signal Process.*, vol. 140, no. 2, pp. 107–113, 1993.

[11] M. A. Nicely and B. E. Wells, "Improved parallel resampling methods for particle filtering," *IEEE Access*, vol. 7, pp. 47593–47604, 2019.

[12] A. Daniyan, Y. Gong, and S. Lambotharan, "An improved resampling approach for particle filters in tracking," in *Proc. 22nd Int. Conf. Digit. Signal Process. (DSP)*, London, U.K., Aug. 2017, pp. 1–5.

[13] Z. He, Y. Ma, and R. Tafazolli, "Posterior Cramer-Rao bound for inertial sensors enhanced mobile positioning under the random walk motion model," *IEEE Wireless Commun. Lett.*, vol. 1, no. 6, pp. 629–632, Dec. 2012.

[14] S. Xu, R. Chen, Y. Yu, G. Guo, and L. Huang, "Locating smartphones indoors using built-in sensors and WI-FI ranging with an enhanced particle filter," *IEEE Access*, vol. 7, pp. 95140–95153, 2019.

[15] H. Bi, J. Ma, and F. Wang, "An improved particle filter algorithm based on ensemble Kalman filter and Markov chain Monte Carlo method," *IEEE J. Sel. Topics Appl. Earth Observ. Remote Sens.*, vol. 8, no. 2, pp. 447–459, Feb. 2015.
[16] C. Xu, J. He, Y. Li, X. Zhang, X. Zhou, and S. Duan, "Optimal estimation and fundamental limits for target localization using IMU/TOA fusion method," *IEEE Access*, vol. 7, pp. 28124–28136, 2019.
[17] P. Doerschuk, "Cramer-Rao bounds for discrete-time nonlinear filtering problems," *IEEE Trans. Autom. Control.*, vol. 40, no. 8, pp. 1465–1469, Aug. 1995.

Xinxin Wang is currently pursuing the master's degree with the Data and Cyber-Physical System Laboratory (DCPS), University of Science and Technology Beijing. His research interests include wireless localization, multirobots networks, and the Internet of Things.

Cheng Xu (Member, IEEE) received the B.E., M.S., and Ph.D. degrees from the University of Science and Technology Beijing (USTB), China, in 2012, 2015, and 2019, respectively. He is currently an Associate Professor with the Data and Cyber-Physical System Laboratory (DCPS), USTB. He was supported by the Postdoctoral Innovative Talent Support Program from Chinese Government in 2019. His current research interests include swarm intelligence, multirobots networks, wireless localization, and the Internet of Things. He is an Associate Editor of the *International Journal of Wireless Information Networks*.

Shihong Duan received the Ph.D. degree in computer science from the University of Science and Technology Beijing (USTB). She is currently an Associate Professor with the School of Computer and Communication Engineering, USTB. Her research interests include wireless indoor positioning, human gesture recognition, and motion capture.

Jiawang Wan received the B.E. degree from the University of Science and Technology Beijing, China, in 2017, where he is currently pursuing the Ph.D. degree. His research interests include wireless localization, swarm intelligence, and the Internet of Things.